

# Simulation of large-scale fast neutron liquid scintillation detector<sup>\*</sup>

XING Hao-Yang(幸浩洋)<sup>1</sup> WANG Li(王力)<sup>1</sup> ZHU Jing-Jun(朱敬军)<sup>1</sup>  
TANG Chang-Jian(唐昌建)<sup>1</sup> YUE Qian(岳骞)<sup>2;1)</sup>

<sup>1</sup> School of Physical Science and Technology, Sichuan University, Chengdu 610041, China

<sup>2</sup> Department of Engineering Physics, Tsinghua University, Beijing 100084, China

**Abstract:** Neutron background measurement is always very important for dark matter detection due to almost the same effect for the recoiled nucleus scattered off by the incident neutron and dark matter particle. For deep under-ground experiments, the flux of neutron background is so low that large-scale detection is usually necessary. In this paper, by using Geant4, the relationship between detection efficiency and volume is investigated, meanwhile, two geometrical schemes for this detection including a single large-sized detector and arrayed multi-detector are compared under the condition of the same volume. The geometrical parameters of detectors are filtrated and detection efficiencies obtained under the similar background condition of China Jinping Underground Laboratory (CJPL). The results show that for a large-scale Gd-doped liquid scintillation detector, the detection efficiency increases with the size of detector at the beginning and then trends toward a constant. Under the condition of the same length and cross section, the arrayed multi-detector has almost similar detection performance as the single large-sized detector, while too much detector number could cause degeneration of detection performance. Considering engineering factors, such as testing, assembling and production, the 4×4 arrayed detector scheme is flexible and more suitable. Furthermore, the conditions for using fast and slow signal coincidence detection and the detectable lower limit of neutron energy are evaluated by simulating the light process.

**Key words:** neutron, large-sized, liquid scintillation detector, Monte Carlo simulation, Geant4

**PACS:** 24.10.Lx, 29.40.Mc **DOI:** 10.1088/1674-1137/37/2/026003

## 1 Introduction

The main candidate of dark matter, weakly interacting massive particle (WIMP), can be detected through elastic scattering with a nucleus in a detector, which is similar to the interaction of a neutron (neutrons can produce nuclear recoils in the same way as WIMPs). For this reason, the measurement of neutron background is very important for the direct detection experiments of dark matter. CJPL is the first deep underground laboratory in China, which is located in one of several tunnels of Jinping Mountain in Sichuan Province. CJPL has approximately 2400 meters of marble overburden, which means better shielding than any other underground laboratory in the world [1]. The muon flux in CJPL is much less than the level of the ground and will not be a main background source of dark matter experiment in CJPL. So the background radiation in CJPL mainly consists of gamma rays and neutrons, both of which can come from the radioactive isotopes in rocks and secondary interactions induced by cosmic-ray muons. One characteristic

of neutrons from these sources is their wide energy range. Besides spontaneous fission of <sup>238</sup>U, ( $\alpha$ , n) reactions are also initiated by particles from U/Th decay chains in the rock and muon induced radioactive nuclei. The energy spectra of emitted neutrons in ( $\alpha$ , n) reactions are quite uncertain. Another characteristic of neutrons at the underground laboratory is that their flux is usually so small that it requires measurement with a relatively large-scale detector.

A typical tool of fast neutron detection is a Gd-doped liquid scintillation detector due to its good discrimination of gamma background with the coincidence of the signals of hydrogen recoil and thermalized neutron capture by the Gd isotope. For the requirement of large scale, two strategies were put forward herein for choice. One is the arrayed liquid scintillation neutron detector [2–5], the other one is a single large-sized detector (or named as whole-body detector) [6–9]. To offer a suitable scheme to measure the fast neutron background in CJPL, a simulation work based on Geant4 is implemented to give an optimized design. The present paper focuses on

Received 9 April 2012, Revised 19 June 2012

<sup>\*</sup> Supported by National Natural Science Foundation of China (10935005, 10945002)

1) E-mail: yueq@mail.tsinghua.edu.cn

©2013 Chinese Physical Society and the Institute of High Energy Physics of the Chinese Academy of Sciences and the Institute of Modern Physics of the Chinese Academy of Sciences and IOP Publishing Ltd

improving detection efficiency by using simulation and comparing two different constitution strategies of large-scale neutron detector. Physical processes in simulation include the incidence of neutrons, propagation of recoiled hydrogen nuclei, the capturing of thermal neutrons and photon releasing.

## 2 Simulation of interaction of liquid scintillator and neutrons

The liquid scintillator is the main component in a liquid scintillation neutron detector. In our plan a new gadolinium-doped liquid scintillator was considered to be adopted, which was developed by the Institute of High Energy Physics (IHEP) of the Chinese Academy of Sciences and named Daya Bay liquid scintillator (D-LS) herein. This D-LS has relatively higher scintillation light yield and higher stability than other similar products, and has been applied in the detection of reactor neutrinos by Daya Bay Collaboration [10, 11]. The Gd-doped liquid scintillator has two advantages. First, isotopes  $^{155,157}\text{Gd}$  have a large thermal neutron capture cross section which can shorten the neutron capture time. Second, a high-energy ( $\sim 8$  MeV) gamma cascade was released after thermal neutron capture by  $^{155,157}\text{Gd}$  nucleus and the amplitude of the Gd-captured neutron signal will be usually larger than that from the natural radioactive gamma backgrounds. In order to study the characteristics of the neutron capture signal by D-LS and demonstrate the accuracy of our Monte Carlo simulation program, we simulated the energy response of D-LS to the captured neutrons by using a Geant4 simulation program.

According to the description of the prototype D-LS detector constructed for the Daya Bay neutrino experiment in Ref. [11], we have simulated the calibration of the prototype detector with Pu-C neutron source. In our program the simulated detector consists of an acrylic tank inside a stainless steel tank. The acrylic tank was filled with 0.5 ton liquid scintillator. A plutonium-carbon (Pu-C) neutron source was located at the center of the detector. The scintillator base is linear alkyl benzene (LAB), Carboxylic acid 3, 5, 5-trimethylhexanoic acid is used as complexing ligand to form organo-complex with gadolinium chloride, and 2, 5-diphenyloxazole (PPO), and 1, 4-bis [2-methylstyryl] benzene (bis-MSB) are used as primary fluor and wavelength shifter, respectively. The mass ratio of C, H, N, O and Gd of this scintillator is 0.8535:0.1288:0.0003:0.0164:0.0010 [11].

Figure 1 shows the comparison of the simulation and experimental data. The solid curve is our simulation result and the experimental data are from Ref. [10]. From the figure, it shows that the two obvious peaks correspond to the neutron captured by H and Gd, whose en-

ergy is  $\sim 2.2$  and  $\sim 8$  MeV, respectively. In the high energy part the spectrum shows good agreement between data and simulation, and in the low energy part the simulation conforms to the data approximately except for the difference around the 400 channel. Analyzing indicates the difference probably comes from the fluctuation of the trigger threshold of the data acquisition system (DAQ) in experiments.

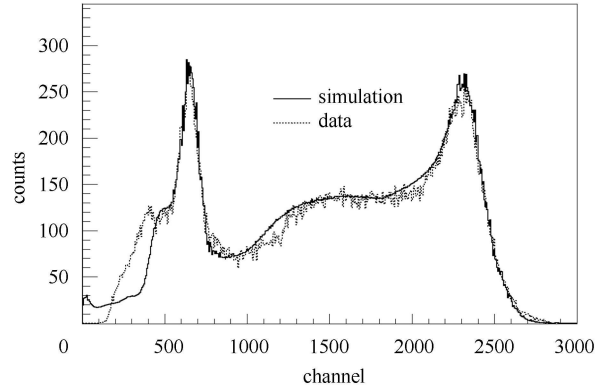


Fig. 1. Neutron spectrum captured by H and Gd when the Pu-C source is located at the center of the Gd-doped liquid scintillator prototype detector.

This result shows that our programming and parameter configuration in Monte Carlo simulations using the GEANT4 toolkit can describe the experimental results of D-LS, especially in the high energy part, and it is able to reproduce the response process of neutrons.

## 3 Geometrical design of large-scale liquid scintillator detector

The large scale liquid scintillator was designed based on the principle of higher detection efficiency, better neutron-gamma ( $n-\gamma$ ) discrimination capability and ease of fabrication. To record an effective neutron event, coincidence detection was adopted in simulation.

When a neutron enters the liquid scintillator detector, it would collide with a proton, then slow down and the thermalized neutron is captured by the Gd nucleus. The energy of the recoiled proton and the gammas from the neutron captured by Gd will deposit in the scintillator detector and induce a light pulse. In this process, the ionization and excitation of the recoiled proton produce a prompt signal and the gammas from the process of the neutron captured by the Gd nucleus produce a delayed signal.

An effective neutron event has to be confirmed by the coincidence of both fast signal and slow signal and this coincidence method can effectively get rid of the background of gamma. This judge standard was adopted in the next design method. According to this standard, the

detection efficiency is defined as the ratio of the number of detected neutrons to the number of neutrons which get into the detector. A similar concept used in the later work is the ratio of detection, which is defined as the number of detected neutrons divided by the total number of incident neutrons in experimental space. Comparing with the former, the surface areas factor is considered in the latter.

### 3.1 Response of detection efficiency to size of detectors

For a cubic detector, if the size increases, the total cross section will increase too. But it will not definitely lead to the increase of the detection efficiency.

According to the transformation efficiency of the liquid scintillator, energy deposition of 50 keV is set to be the threshold of detection [6]. An effective detection event is determined by the fast signal and slow signal when they pass through the 50 keV energy threshold at the same time. Detection efficiency is defined as the ratio of the event number of detected neutrons to the number of neutrons that strike into the detector.

To find a suitable volume of the large scale detector, different volumes of the cube are assigned in a simulation whose length on each edge varies from 200 mm to 1400 mm. The neutron enters the detector along the central axis of one side of the cube and the energies of incident neutrons are 1 MeV, 5 MeV and 10 MeV respectively.

Figure 2 shows that the detection efficiency increases obviously with the size of detector at the beginning and then trends to a constant value. From 200 mm to 400 mm, the detection efficiency changes sharply with the side length. Afterwards the increase becomes slow. When the length of one edge of the cube increases to 1000 mm, the detection efficiency is almost the same. It can be seen that the changes of detection efficiency with length are different for different neutron energies. The detection efficiency of higher energy neutron varies sharper than that of lower energy neutrons.

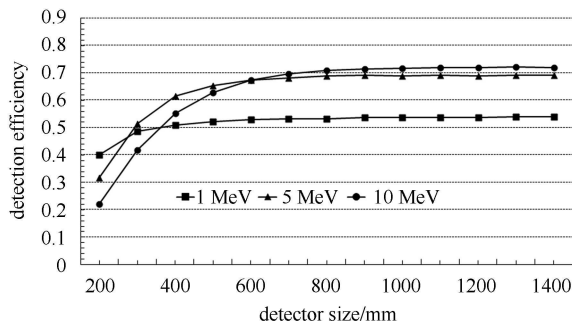


Fig. 2. Detection efficiencies of cube detectors of different sizes.

Since the cylinder is more convenient than the cube from the view of construction, and the photomultipliers

(PMTs) usually are fixed on the two ends of cylinder, the effect of detector length on detection efficiency needs to be evaluated. Simulations of cylinder detectors whose cross section diameters are one meter and lengths vary from 200 mm to 1400 mm are executed with the same method and configuration of the former simulation.

Figure 3 shows that the detection efficiency changes of cylinder detectors of different lengths are similar to the changes of cube detectors of different sizes. At the beginning, the detection efficiency increases with the detector length obviously, and then the detection efficiencies change gently. The reason for this trend is that when the volume of the detector reaches a certain value, all the neutrons except those rebound from the incidence plane can be captured by the nucleus in the scintillator, among them the ratio of neutrons to be captured by Gd is a constant [12], so the detection efficiency trend is to be a fixed value.

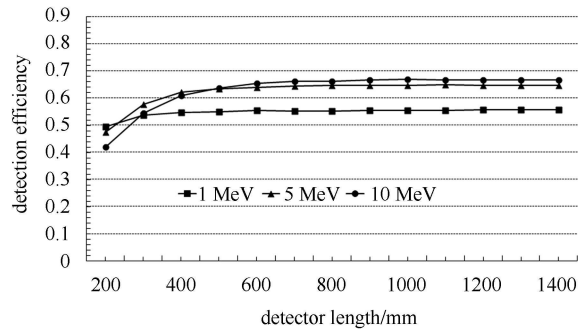


Fig. 3. Detection efficiencies of cylinder detectors with different lengths.

Linking the above conclusions, for a fixed cross section cylinder of one meter diameter, a suitable length is also one meter.

### 3.2 Analysis of influencing factors on detection efficiency

It is a general rule that a larger volume is more helpful for the trapping of thermal neutron in a liquid scintillator. However, because the coincidence detection principle is adopted here, we give more consideration to the factors involved in the recoiling process and Gd capturing.

Since the fast signal and slow signal occur at different positions, in order to cover the area where the thermal neutron is captured by Gd, simulations are implemented to make certain the distribution range of neutron capturing. In this part of the simulation a neutron detector whose size is 1 m×1 m×1 m is used. No container or shell is considered in this simulation. The kinetic energy here is set to be 10 MeV. In a hall deep underground in CJPL, the cosmic-ray muons are so few that the flux of a muon-induced neutron is less than the flux of a neutron

from ambient natural radioactive isotopes and spontaneous fission. So the 10 MeV neutron can be regarded as a typical high energy neutron in our experiment. The incident neutron is emitted from the center of one surface and goes along the symmetrical axis and the coordinates where the neutron collides with a proton or other nucleus and the neutron is captured by Gd are recorded.

Figure 4 (a), (b) and (c) show the distribution of locations where the first collision and Gd capturing take place from stereo view, side view and front (incident

point) view. The red spot denotes the position where the first collision takes place, and the blue spot means the position where the capturing takes place. From Fig. 4(b), it can be seen that the incident neutrons collide with protons along the incident direction and the range from edge to depth is about 600 mm. The blue spots show that the site of thermal neutron capturing by the Gd nucleus is mainly takes place around the area near the incident point of the neutrons. Most (Gd, n) captures are located in the space 600 mm×600 mm×600 mm.

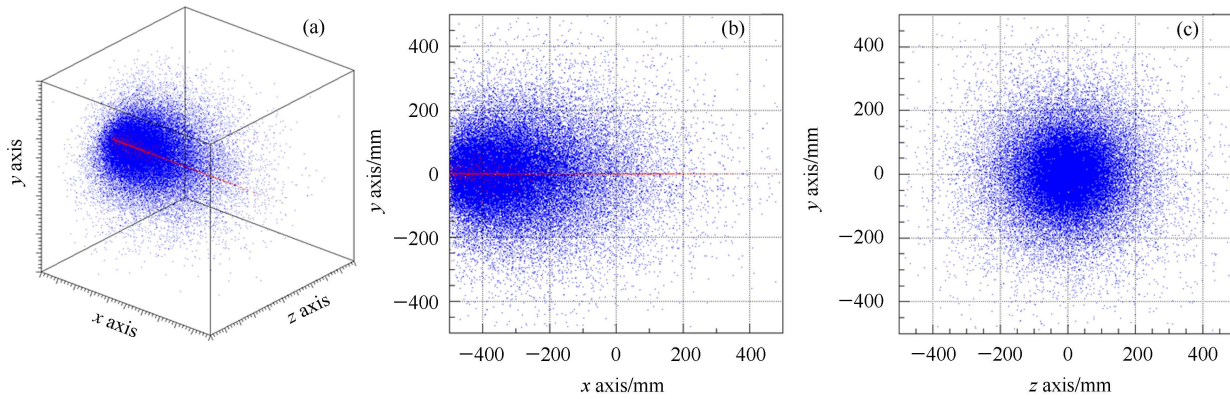


Fig. 4. (color online) Locations of neutron collision with proton first (Red) and Gd capturing (Blue).

The kinetic energy of a neutron is lost continually when it collides consecutively with different nuclei and is captured by a Gd nucleus when thermalized finally. In this process, a neutron will travel a certain distance. The distribution of the distance in simulation is shown by the blue spot in Fig. 4. From Fig. 5, one can see that the main Gd capturing occurs at around 100 mm away from the location of the first collision. The longest distance between them is about 800 mm.

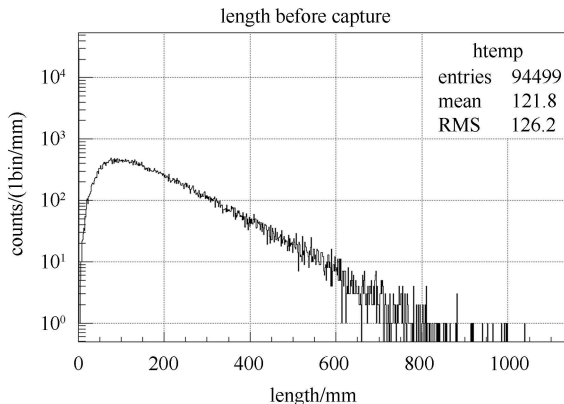


Fig. 5. Distance distribution of the n-p collision and (Gd, n) capture.

In simulations of this section, we do not consider the total detection cross section which would increase with

volume. The real scale of the detector depends on the requirement of the measurement of the lowest limit of neutron flux. Combining the detection response and locations where nuclear recoiling and Gd capturing occur the volume of the detector is assigned to be 1 m<sup>3</sup> in our plan. In the next step, different structural schemes are used to investigate their corresponding change of detection efficiency in a real experiment surrounding to get an optimized geometrical structure of the large scale detector.

### 3.3 Detection efficiency comparison of two schemes

As mentioned before, the expected detectors in this experiment are cylinder-shaped. The whole-body detector or the unit of the arrayed detector is designed to be a tube. It consists of a cylindrical OFHC(oxygen-free highly-conductive copper) vessel, which will be connected at each end by a PMT through quartz windows in the future.

When the total volume of the detector is given, the large-scale detector can be a whole-body detector or a detector array. For the arrayed detector, there are several different combination patterns for different cross sections of the detector unit on the condition of fixed volume. In this paper, five patterns are proposed for evaluation.

They are the whole-body detector, the  $2 \times 2$  detector array, the  $3 \times 3$  detector array, the  $4 \times 4$  detector array and the  $5 \times 5$  detector array. Fig. 5 shows the structure of the two strategies of large scale liquid scintillator detector. Fig. 6(a) is a whole-body detector. Fig. 6(b) shows the  $3 \times 3$  detector array as an example, the same nine detector units fill the  $1 \text{ m} \times 1 \text{ m} \times 1 \text{ m}$  spatial volume. Other array schemes have similar structure: for the  $2 \times 2$  detector array, there are four detector units with a diameter of 500 mm; for  $4 \times 4$ , sixteen units (diameter 250 mm); and  $5 \times 5$ , twenty-five units (diameter 200 mm). All the sizes listed in brackets do not include the thickness of the detector shells.

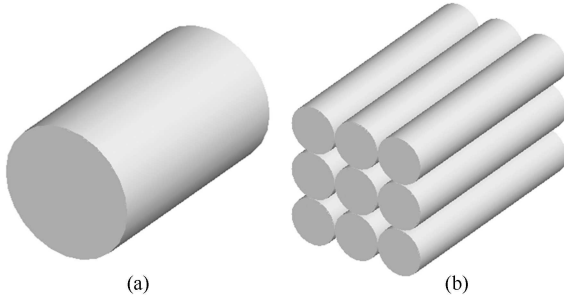


Fig. 6. The structures of two schemes, the  $3 \times 3$  arrayed detector and the whole-body detector.

In this part, simulations about the five schemes are done under the same condition to compare their performance. The incident neutrons are generated at any point of the inner surface of the experiment room, with a random inward direction. The inner space of the room is  $4 \text{ m} \times 4 \text{ m} \times 4 \text{ m}$ . The energy of the incident neutrons is sampled according to the neutron background energy spectrum of a typical underground laboratory, which can be chosen to be the substitution of the real neutron spectrum in CJPL [13] and mainly comes from the decay chains of U and Th isotopes in rocks and concrete around the lab.

According to these data and the principle of an effective neutron detection event discussed in Section 3.2, we have calculated the number of neutrons detected and the detection efficiency of the detectors. We have also defined a ratio of detection as the number of neutrons detected divided by the total number of incident neutrons from the inner surface of the experiment room.

Figure 7(a) shows the detection efficiency of the five schemes and Fig. 7(b) shows the ratio of detection. As the number of units increases, it can be seen that the detection efficiency decreases a little bit. For the ratio of detection, it increases at first and the  $4 \times 4$  detector array has the largest ratio of detection. The greater the number of units the detector has, the more the surface-volume ratio (the ratio of total surface area of all detectors to the fixed total volume) and the structural material (detector shells) it will have. It can be seen that the

surface-volume ratio is also an important factor which can affect the detection performance.

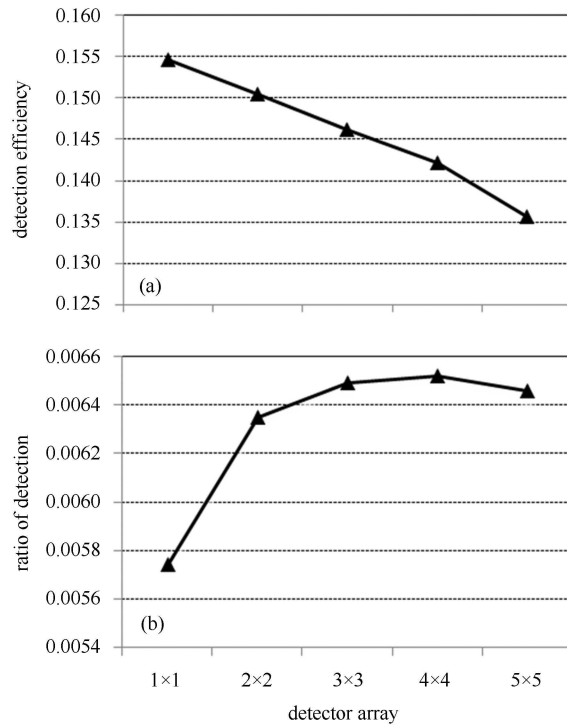


Fig. 7. The detection efficiency and ratio of detection of five schemes.

## 4 Simulation of light emission process

The simulations of the fluorescent light emission process in the large-scale liquid scintillator detectors are presented in this section. Simulations include light pulse shapes which are produced by the incident neutron and gamma, light collection efficiencies for the detectors whose diameter are 250 mm and 1000 mm respectively. The inner surface of the tubal vessel is coated with Teflon for light reflection. The liquid scintillator is the same as the former one in Section 2. In Geant4 we use 'UNIFIED' model to simulate the behavior of photons at medium boundary. The UNIFIED model can deal with all aspects of surface finish and reflector coating. It provides a realistic simulation of the optical interfaces.

### 4.1 n- $\gamma$ light pulse simulation

The capability of n- $\gamma$  pulse-shape discrimination is an important aspect for evaluation of the performance of liquid scintillators. Light pulses from the interaction of the incident neutron and the liquid scintillator, the gamma photon and the liquid scintillator are generated by using different configurations for the fast and slow time constants of the scintillator. Photon generations, photons arrived at a sensitive area with time are

recorded to form pulse waveform. The sensitive areas are set to be two ends of 250 diameter and 1000 diameter liquid scintillator tubes. Both incident neutron and gamma energy are 10 MeV and the amplitudes of the pulses are normalized to the same level to compare the pulse waveforms.

Figure 8 shows that the light output waveforms produced by the incident neutron and the gamma photon resemble each other. This result also confirms that the fast and the slow deposit signal coincidence is necessary for an effective detection event. Simulations of light pulses of different neutrons and gammas at different energies are also executed. Their pulse shapes do not have obvious difference after amplitude normalization.

Coincidence detection here depends on two independent signals, the fast and slow signal. The duration time between the fast signal and the slow signal is approximately an exponential distribution, which is shown in Fig. 9. It can be seen that almost 90% of the slow signals take place within 200  $\mu\text{s}$ , so a suitable time delay window after the first signal should be 200  $\mu\text{s}$ .

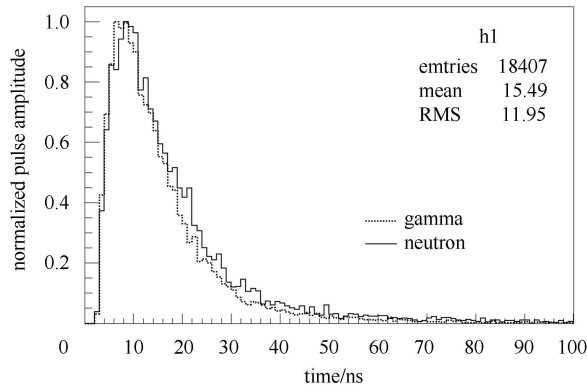


Fig. 8. Light pulse waveform comparison of neutron and gamma in one PMT (Normalized amplitude).

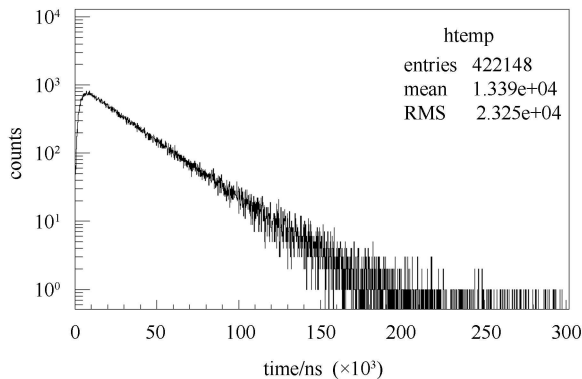


Fig. 9. Duration time between fast signal and slow signal.

However, during the 200  $\mu\text{s}$ , a gamma photon probably enters the detector and causes a detection event and

this event can lead to a mistake in judgment of neutrons. This means that a reliable fast-slow coincidence detection needs to decrease the gamma flux to a lower flux. To satisfy this condition, a copper shell should be adopted to shield gamma. Here copper is chosen to be the shielding material for its low radio background. In a typical underground laboratory the gamma background energy are under 3000 keV, 99% of their energies are between 0 and 500 keV, especially concentrated around 100 keV, and their corresponding flux is  $0.28 \text{ cm}^{-2}\text{s}^{-1}$  [14]. According to this flux and the cross section of gamma, the event number in the scintillator during 200  $\mu\text{s}$  from the background gamma is around two. It is quite possible to produce a false fast-slow coincidence event. According the attenuation coefficient of gamma in copper, a suitable shield layer is 40 mm, which can decrease the detection of pseudo-events of neutrons to a 1% level of the original value.

#### 4.2 Light collection and detectable energy lower limit

A signal of PMT comes from the photons which can reach the photocathode. For a detection system based on light signals, the light collection is important. With the multiple reflection and propagation in the liquid scintillator, some of the photons are absorbed by the medium before they get to the ends of the liquid scintillator tube. On the other hand, the tubular shape detector is designed to perform two-end coincidence detection by using two PMTs fixed on its two ends. In this case, the produced scintillation light which is transmitted to the photodetector can be divided into the left and right components. The intensity of the two components can be affected by the location where the particle is incident, which also means that a different incident location can cause different light pulse amplitude.

Figure 10. shows the light pulses of two components of photons from proton recoils induced by neutron elastic scattering under the condition where the neutron is incident at one end of the detector (a) and the middle of the detector (b) (250 mm diameter). The solid curve is the light pulse waveform, the dotted curve is the light pulse that arrived at one end of the detector and the broken curve is the light pulse that arrived at the other end of the detector (in Fig. 10(b)); to demonstrate the two pulses clearly, blue and red curves are used to draw the waveforms of the pulses. From Fig. 10 it can be seen that there is a time delay between two pulses, while the time delay is too short to impact the coincidence time configuration. On the other hand, the areas under light pulses contain information about the light collection efficiencies. The light collection efficiency is a ratio of the photon number entering the sensitive area to the number of photons generated by the liquid scintillators, which

can be expressed by the ratio of the area of PMT pulse waveform to the area of the total light pulse waveform. The light collection efficiencies at the two ends are different, especially in the extreme condition where a neutron is incident near to the end of the detector. In this condition, due to the low collection efficiency, the number of photons which get to the opposite end of the tubular detector is probably not enough to produce an effective signal, and only one end PMT of the detector can give a signal. This case leads to an event being lost in the two-end coincidence detection, while it can prohibit the false events due to PMTs and DAQ systems.

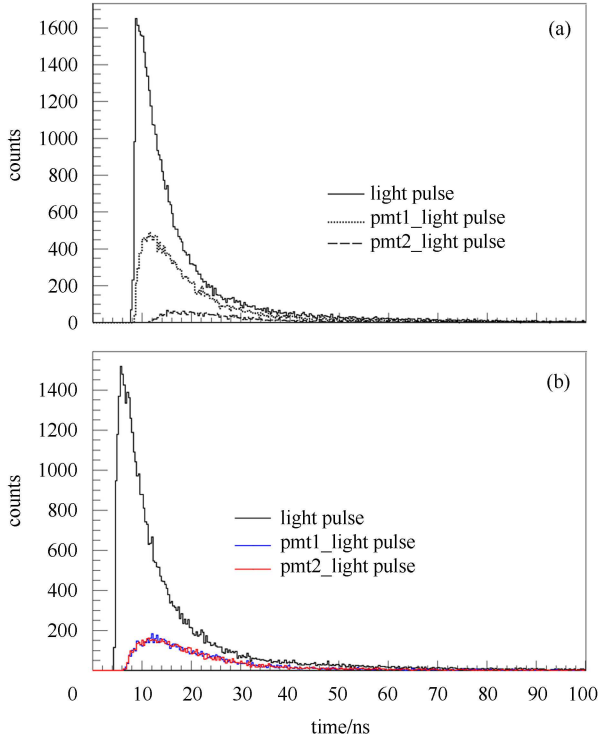


Fig. 10. (color online) (a) Waveforms of the light pulse drawn by recording photon generation in the scintillator and waveform of light pulses drawn by recording the photon number that arrived at each end of the detector when a neutron hit one end of the detector unit; (b) Waveforms of the light pulses drawn in the same way with (a) when a neutron hit the middle part of the detector unit.

Another factor to impact the signal generation in the extreme condition is the energy of the incident particle, which can affect the produced photon number. Here the lowest energy requirement in the extreme condition is evaluated from simulations. To produce an effective signal output from PMT, the photon number during one pulse width should be more than 20 according to the PMT quantum transform efficiency in the normal condition. An effective output ratio (the number of effective output to the number of total output) is used to evaluate

the effective light pulse output of neutrons at different energy. The dotted line in Fig. 11 represents the effective output ratio when a neutron enters the detector from the near-end; a smaller energy can produce an effective output. However the solid line shows that if the neutron enters the detector from the far-end, when the incident energy is smaller than 0.5 MeV, the probability of producing an effective signal is smaller than 50%. In this approach, the effective lower limit of energy of neutron detection can be 0.5 MeV.

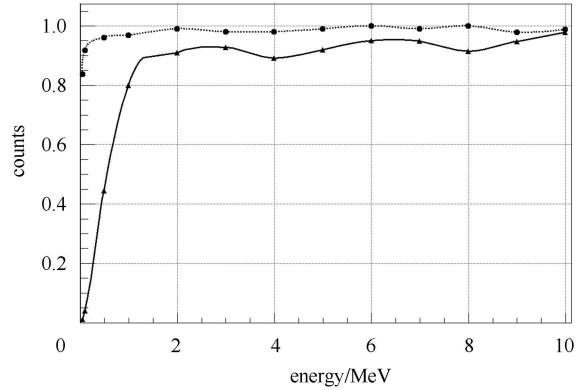


Fig. 11. Count rate of neutrons at different energy; the solid line is the relative count ratio of the far-end of detector, the dotted line is the one of near-end.

## 5 Summary

The measurement of neutron background is an important work for dark matter experiments. A detailed simulation about the Gd-doped liquid scintillator neutron detector was performed for the design of the real detector. According to the relationship between detection efficiency and detector size, the range of n-p collision and (Gd, n) capturing, a suitable size for the detector is 1 m×1 m×1 m for the detection of the fast neutron with energy less than 10 MeV. Furthermore, a comparison of single large size detector strategy and arrayed detector strategy was done to give a better choice for the shape of detector. The result shows that both of them have similar results, splitting the volume into an array does not degenerate its performance. For the detection efficiency, the whole-body detector is a little higher, while for the ratio of detection the arrayed detector is a little better due to the larger surface-volume ratio. The ratio of detection increases with the detector number, but too many units (such as 5×5) in a detector array produces a lower ratio of detection than others for the reason that shells would occupy a larger space and decrease the probability of Gd capturing.

Further simulations about light processes in a liquid scintillator were also done in this work. These simula-

tions prove that the fast slow signal coincidence is reasonable for the relatively inferior capability of pulse shape distinguishing. Meanwhile, the requirement of a gamma background shield was given initially. For the two-end coincidence detection, the detectable lower energy limit was estimated according to the simulation data. Considering more factors in engineering synthetically, including

operability, flexibility, and convenience of maintenance, we believe that a  $4\times 4$  arrayed detector whose volume is one  $\text{m}^3$  is more practical than the others. So in the next step a Gd-doped liquid scintillator detector as the proposed strategy is going to be adopted, which should satisfy the detection requirement of neutron background in CJPL.

## References

- 1 Normile D. *Science*, 2009, **324**: 1246
- 2 Olsson N, Söderman P O, Nilsson L et al. *Nucl. Instrum. Methods A*, 1994, **349**(15): 231
- 3 Deniz M et al. (TEXONO collaboration). *Phys. Rev. D*, 2010, **81**(7): 072001
- 4 Hagner T, Hentig R V, Heisinger B et al. *Astrop. Phys.*, 2000, **14**: 33
- 5 ZHANG J L, TAN Y H, WANG H et al. *Nucl. Instrum. Methods A*, 2010, **623**: 1030
- 6 Tziaferi E, Carson M J, Kudryavtsev V A et al. *Astrop. Phys.*, 2007, **27**: 326
- 7 Chazal V, Brissot R, Cavaignac J F et al. *Astrop. Phys.*, 1998, **9**: 163
- 8 Kozlov V Yu, Armengaud E, Augier C et al. *Astrop. Phys.*, 2010, **34**: 97
- 9 Fisher B M, Abdurashitov J N, Coakley K J et al. *Nucl. Instrum. Methods A*, 2011, **646**: 126
- 10 DING Ya-Yun, ZHANG Zhi-Yong, LIU Jin-Chang et al. *Nucl. Instrum. Methods A*, 2008, **584**: 238
- 11 WANG Zhi-Min, YANG Chang-Gen, GUAN Meng-Yun et al. *Nucl. Instrum. Methods A*, 2009, **602**: 489
- 12 LIU Jin-Chang. *Background Study and Prototype Testing of the Daya Bay Experiment* (Ph. D. Thesis). Beijing: Institute of High Energy Physics, CAS, 2008 (in Chinese)
- 13 MEI D M, ZHANG C, Thomas K et al. *Astrop. Phys.*, 2010, **34**: 33
- 14 Marijke H, Laura B, Tobias B et al. *Nucl. Instrum. Methods A*, 2011, **643**: 36